

Collapse of Showa Bridge Revisited

Subhamoy Bhattacharya, Professor and Chair in Geomechanics, University of Surrey, U.K; email: <u>S.Bhattacharya@surrey.ac.uk</u>

Kohji Tokimatsu, Professor, Tokyo Institute of Technology, Japan; email: kohji@o.cc.titech.ac.jp

ABSTRACT: The collapse of the Showa Bridge during the 1964 Niigata earthquake features in many publications as an iconic example of the detrimental effects of liquefaction. It was generally believed that lateral spreading was the cause of failure of the bridge. This hypothesis is based on the reliable eye witness that the bridge failed 1 to 2 minutes after the earthquake started which clearly ruled out the possibility that inertia (during the initial strong shaking) was the contributor to the collapse. Bhattacharya (2003), Bhattacharya and Bolton (2004), Bhattacharya et al (2005) reanalyzed the bridge and showed that the lateral spreading hypothesis cannot explain the failure of the bridge. The aim of this short paper is to collate the research carried out on this subject and reach conclusions based on analytical studies and quantitative analysis. It is being recognised that precise quantitative analysis can be difficult due to lack of instrumented data. However, as engineers, we need to carry out order-of-magnitude calculations to discard various failure hypotheses.

KEYWORDS: Showa Bridge, Niigata earthquake, collapse, liquefaction.

SITE LOCATION: <u>IJGCH-database.kmz</u> (requires Google Earth)

INTRODUCTION AND THE FAILURE OF SHOWA BRIDGE

The collapse of the Showa Bridge during the 1964 Niigata earthquake features in many publications as an iconic example of the detrimental effects of liquefaction, such as, Hamada and O'Rourke (1992), Kramer (1996), Bhattacharya (2003), Bhattacharya *et al.* (2005), Yoshida *et al.* (2007) and Bhattacharya *et al.* (2008). Figure 1 shows a photograph of the failure of the bridge following the 1964 Niigata earthquake. The Niigata earthquake occurred on the 14th of June 1964 and registered a moment magnitude of 7.6. The bridge is located about 55 km from the epicentre, crossing the Shinano River. The bridge was a three month old steel girder bridge supported on pile foundations and was one of the many bridges over Shinano river (i.e. Bandai and Yachiyo bridge) which collapsed as a result of the earthquake. The total length of Showa bridge was about 304 m and had 12 composite girders having a breadth of about 24 m. The main span length was about 28 m and side span length was about 15 m (Fukuoka 1966).



Figure 1. Collapse of Showa Bridge.

It is interesting to observe that the middle of the bridge i.e. the bridge piers collapsed while the abutments (end piers) remained stable. Figure 2 shows the ground profile along the longitudinal direction of the bridge following Hamada and

Submitted: 02 June 2013; Published: 26 August 2013

Reference: Bhattacharya, S., and Tokimatsu, K. (2013). Collapse of Showa Bridge Revisited.

International Journal of Geoengineering Case histories, http://casehistories.geoengineer.org, Vol.3, Issue 1, p.24-35.

doi: 10.4417/IJGCH-03-01-03



O'Rourke (1992). It was generally believed that lateral spreading was the cause of failure of the bridge (see for example the seminal work of Hamada and O'Rourke (1992) collating the performances of infrastructures following the major earthquakes in United States and Japan). In other words, the hypothesis was based on the fact that lateral pressure of the liquefied soil pushed the pile sideways to cause the pile to fail in bending. This hypothesis is based on the reliable eye witness that the bridge failed 1 to 2 minutes after the earthquake started which clearly ruled out the possibility that inertia (during the initial strong shaking) was the contributor to the collapse. Figure 3 shows the longitudinal section of the river along with the pile displacement profile following the earthquake.

Bhattacharya (2003), Bhattacharya and Bolton (2004), Bhattacharya *et al* (2005) reanalysed the bridge and showed that the lateral spreading hypothesis cannot explain the failure of the bridge. It was argued that had the cause of failure been due to lateral spreading, as suggested, the piers (see Pier P5 and Pier P6 in Figure 3) should have displaced identically in the direction of the slope. Also the piers close to the riverbanks did not fail, where the lateral spreading was observed to be severe.

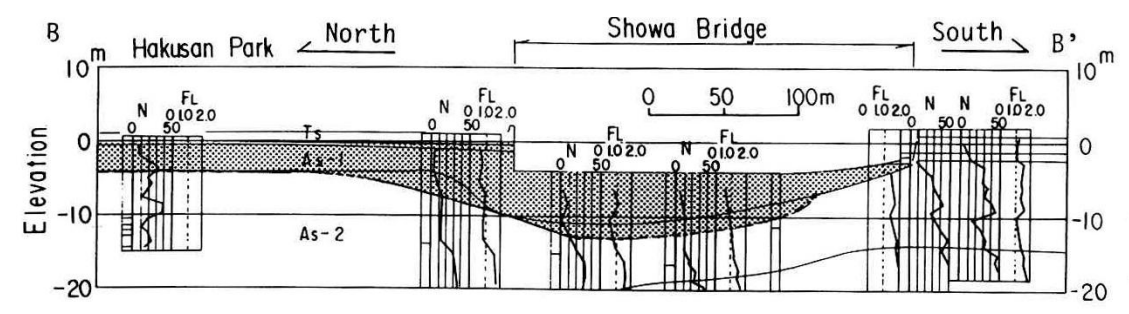


Figure 2. Soil liquefaction profile (in grey), Hamada and O'Rourke (1992).

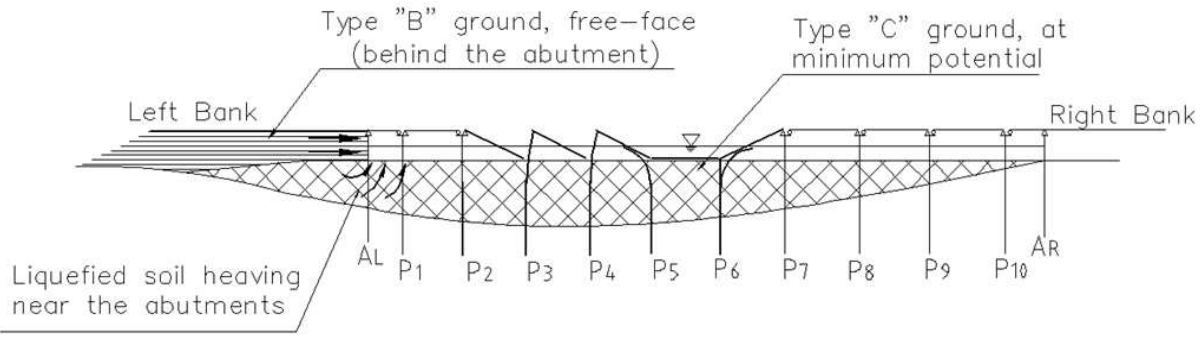


Figure 3. Liquefaction profile at Showa Bridge divided into ground types as defined by Hamada et al. (1986) cases (B) and (C). The soil profile has been adapted from Hamada (1992).

This conjecture that the bridge did not fail by lateral spreading was later confirmed by Yoshida *et al.* (2007) who carried out a detailed survey to ascertain the most likely time of collapse of the bridge i.e. the onset of the falling of the decks. The main conclusion reached by the authors is that lateral spreading of the surrounding ground started at about 83 seconds when the bridge had already collapsed. Bhattacharya *et al* (2004) proposed a hypothesis that as soil liquefies, the pile loses the lateral restraint in the zone of liquefaction and behaves like an unsupported column prone to buckling instability. Essentially, the pile in the zone of liquefaction behaves as an axially loaded column rather than laterally loaded beams. In other words, the axial load effects on the pile cannot be ignored.

The aim of this short paper is to collate the research carried out on this subject and reach conclusions based on analytical studies and quantitative analysis. It is being recognised that precise quantitative analysis can be difficult due to lack of instrumented data. However, engineers need to carry out order-of-magnitude calculations to discard various failure hypotheses.



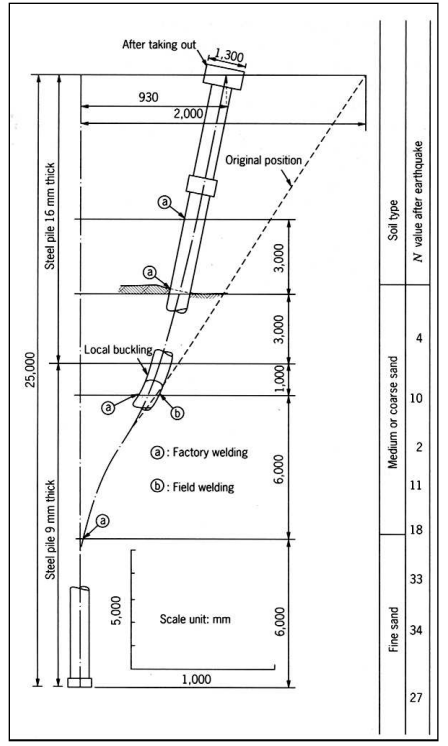


Figure 4. Deformed shape of a recovered pile (P4 as shown in Figure 3) after the earthquake. The original shape refers to the position just after the earthquake, Fukuoka (1966).

IMPORTANCE OF INCLUSION OF EFFECTS OF AXIAL LOAD ON BENDING RESPONSE OF THE PILE

In field condition, piles are subjected to both axial and lateral loads during earthquakes, and they are therefore better considered as beam-column elements rather than laterally loaded beams. During liquefaction, the buckling load capacity (P_{cr}) of the pile decreases and may be estimated by Equation 1 where EI is the bending stiffness of the pile. On the other hand, L_{eff} is the effective length of the pile in the liquefiable zone and is a function of boundary condition of the pile at the top and bottom of the liquefiable zone and depth of liquefiable zone. A table for calculating the effective lengths of pile can be found in Bhattacharya and Goda (2013).

$$P_{cr} = \frac{\pi^2 EI}{L_{\text{eff}}^2} \tag{1}$$

Considering the static load of the pile (P) as a constant value throughout, if P_{cr} reaches close to P, the structure can suffer excessive bending due to even a very small amount of lateral loading or imperfection. On the other hand, the lateral deflection or bending moment in pile due to lateral loading is expected to increase with decreasing P_{cr} (i.e. increasing P/P_{cr} ratio).

The interaction between the axial and lateral load is generally referred to as P-delta effect. Stability analysis of elastic column (Timoshenko and Gere, 1961) shows that the lateral deflection (y_0) due to lateral loads is amplified in the presence of axial load (P) producing a final deflection of pile (y) as given in equation (2), which is also plotted in Figure 5.

$$\frac{y}{y_0} = \frac{1}{1 - \frac{P}{P_{cr}}} \tag{2}$$

The ratio y/y_0 , commonly known as "Buckling Amplification Factor" (BAF), is a function of the critical buckling load, which depends on the boundary conditions of the pile.



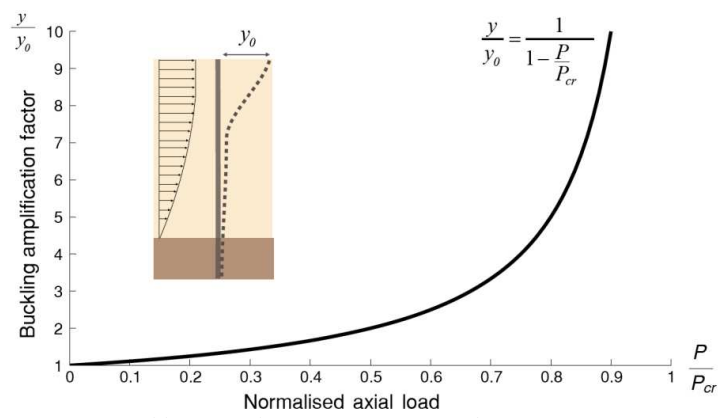


Figure 5. Buckling amplification factor for different ratios of P/Pcr.

For piles subjected to lateral spreading the value of y_0 , due to the lateral load only, may be assessed considering two different methods: (a) Force based method; (b) Displacement based method. Figure 6 shows these two methods of representing a field condition. In force based method, the force from liquefied soil flow is represented by a limiting pressure (F_{max}) on pile. (see Figure 6b). Figure 6c illustrates displacement based method, where the lateral spreading is modelled by applying a displacement at the free ends of the soil springs. Typical results of pile response from these two methods with axial load are described in Figures 7 and 8.

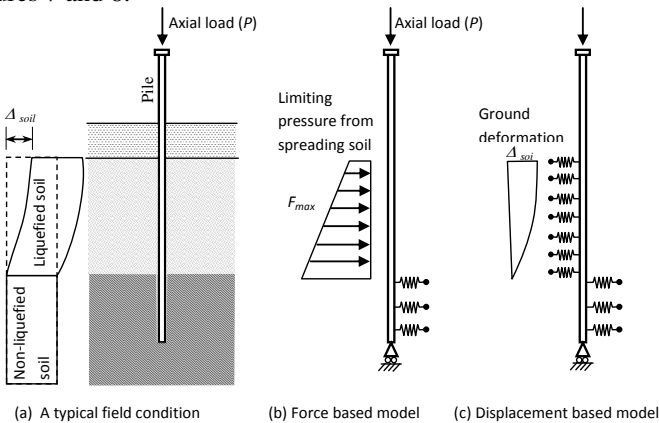


Figure 6. Force and displacement based models of pile-soil interaction in liquefiable soil.

Figure 7 shows the effect of the axial load on the bending response of a pile foundation, in terms of normalized pile displacement y/D (where y is the lateral displacement evaluated considering the effect of axial load) against either Δ_{soil} /D or F/F_{max} depending on the method of analysis (i.e., displacement based method or force based method). Clearly, Figures 7 and 8 show that when the axial load is higher with respect to critical buckling load, the pile head deflection (y) and maximum bending moment in pile get larger.

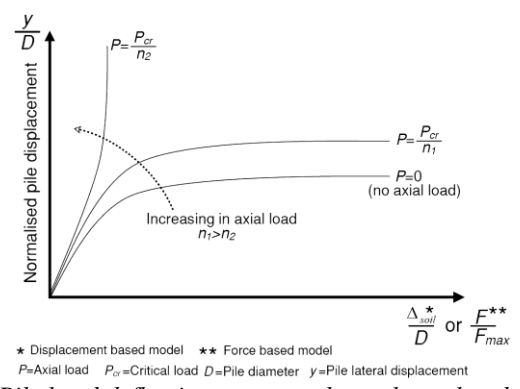


Figure 7. Pile head deflection response due to lateral and axial load.



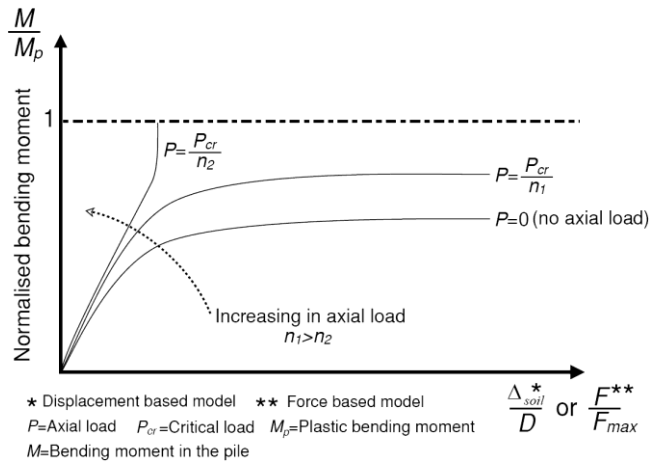


Figure 8. Pile bending moment response due to lateral and axial load.

During liquefaction, as the soil loses its stiffness, the elastic buckling load (P_{cr}) also reduces. Assuming a constant static axial load on pile, this also causes the P/P_{cr} ratio to increase. With the increasing P/P_{cr} , the pile head deflection and bending moment in pile also increase. When this ratio is close to 1, i.e., axial load is close to the buckling load, the bending moment amplification factor becomes very high, which leads the bending moment in pile to reach its plastic moment capacity, M_p , at a lower value of lateral load. The sudden rise in pile head deflection demonstrates the failure of the pile where bending moment reaches M_p and the pile continues to deflect without any additional loading. A similar behaviour can also be observed when the axially loaded piles in level liquefied ground are subjected to inertia loading.

FAILURE MECHANISMS FOR SHOWA BRIDGE

This section of the paper discusses the various failure mechanisms for Showa Bridge. Before the failure mechanisms are discussed, it is necessary to summarize the various loads acting on the pile head during the earthquake. Table 1 shows the axial load acting on the pile under different loading conditions.

Combined Effect of Axial and Lateral Spreading Loads

From the shape of the deformed pile (Figure 4) of the bridge, Berrill and Yasuda (2002) inferred that the movement of the liquefied sand layer towards the river may have caused the deformation of the pile. Figure 9 shows a numerical model to study this effect to verify this aspect. A summary of the analysis is given below:

Table 1. Axial loads for different analysis conditions.

Axial load (P)	Remarks
P=0	Analysis without axial load considerations. This would represent the simplified JRA (2002) procedure.
P=740 kN	The static dead load acting on the pile and any dynamic effects are ignored. This may represent a situation where the earthquake has stopped but the soil is fully liquefied and is flowing laterally past the pile.
P= 370 kN	The static load acting on the pile is half of the dead load. This may represent the condition when one deck has completely dislodged and the lateral flow of soil continues i.e. Pier P_4 in Figure 3 [Yoshida <i>et al.</i> (2007)].

The axial load on each pile can be deduced from the configuration of the Showa Bridge deck. Bhattacharya *et al.* (2005) estimated the static dead load acting on each pile to be 740 kN. The length of the pile in the liquefiable soil zone is about 10 m and the underlying denser non-liquefied sand layer (6 m thick) can be assumed to provide restraint during lateral spreading. The 25 metre pile is therefore subjected to a combination of lateral and axial loads. The pile has been modelled as single standing frame element with lateral nonlinear soil springs at the bottom 6 m to simulate the restraint provided by



the non-liquefied soil layer. The spring constants were obtained from the API (2000) recommendation. The liquefied soil layer is modelled as bi-linear springs which simulate the maximum flow pressure of liquefied soil according to the JRA (Figure 9). Details of the finite element model are shown in Figure 9.

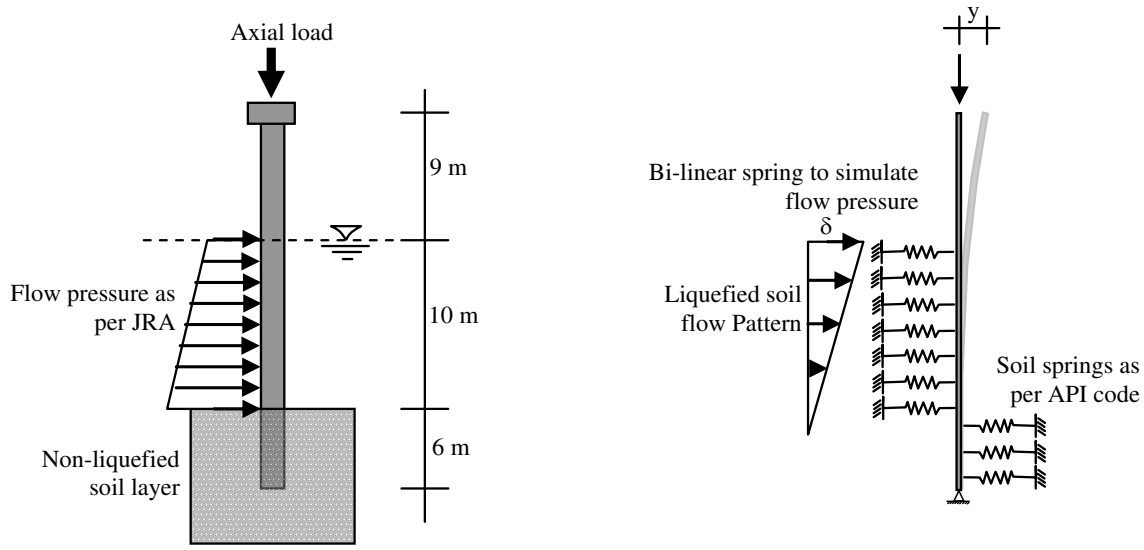


Figure 9. Analysis model for the Showa Bridge pile subjected to lateral soil flow and axial load. (a) Field condition. (b) Numerical model in SAP.

The pattern of the flow of the liquefied soil layer is assumed to have a triangular distribution. SAP2000 was used to perform a nonlinear static analysis for lateral soil flow under the axial loads given in Table 1. In these analyses the beam remains elastic. Figure 10 plots the pile head displacement (y) against the maximum ground deformation (δ) at the top of liquefied soil layer for the different axial loads. When the axial load is omitted (P=0), the pile is pushed over to give a pile tip displacement of about 0.6 m. If the axial load is included in the analysis, the pile tip suddenly becomes unstable (represented by the sharp increase in slope of the curve) at lower ground displacements. For an axial load of 370 kN, corresponding to half the weight of the deck, the pile becomes unstable with a surface lateral ground displacement of about 0.75 m. This figure falls to about 0.2 m when the full weight of the superstructure is applied to the pile. Thus this pile, that appears to be safe under the effect of lateral spreading alone, can fail under the combined action of axial load and lateral spreading.

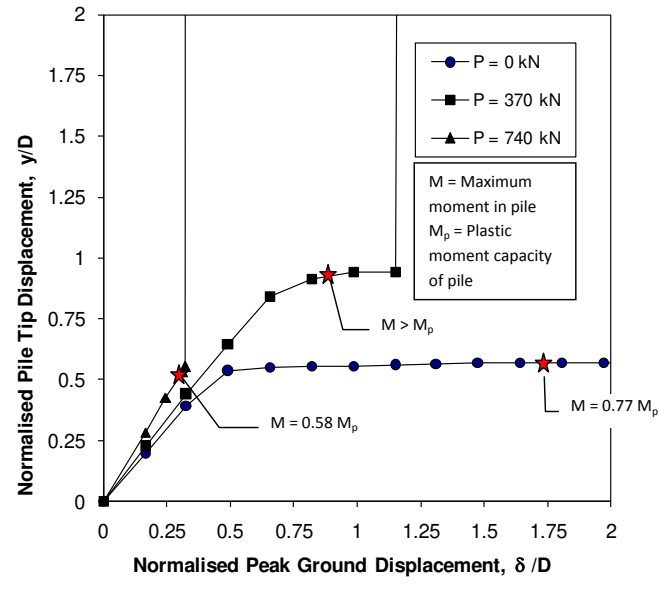


Figure 10. Influence of axial load on pile tip displacement



Whilst it is clear that severe lateral spreading occurred on the left riverbank, there is no evidence that suggests that the riverbed soil (directly underneath the middle of the bridge where the deck fell) was significantly affected by lateral spreading. In fact a potential energy argument can prove the contrary. When the shear stress required for static equilibrium is greater than the shear strength of the soil in its liquefied state, the liquefied soil mass will attempt to flow towards a lower potential energy form. Therefore, liquefied soil on a slope will flow to the bottom of the slope; and, liquefied soil behind a discontinuity (such as a retaining wall) will tend to flow across the discontinuity. As shown in Figures 2 and 3, the liquefied soil of the riverbed (directly underneath the Showa Bridge piers) could not flow laterally because it is already in its lowest potential energy from. It is reasonable to believe that the lateral flow of soil from the left riverbank heaved close to the left abutment (as described in Figure 3), and the soil near piles P_5 and P_6 remained largely stationary. A more detailed discussion can be found in Kerciku *et al* (2008).

The above argument is also supported by the fact that the piers P_5 and P_6 collapsed in opposite directions. Had it been lateral spreading that caused the bending failure of the piles, they would have collapsed in the same direction. Furthermore, Bhattacharya *et al.* (2005) conducted a JRA (1996) code check for bending of piles due to lateral spreading and showed that the bending capacity of the piles is larger than the induced bending moments. Bhattacharya (2003) and Bhattacharya *et al.* (2005) also argued that the piers close to the river banks did not fail, wherein the lateral flow was seen to be severe. Though the combined action of lateral spreading and axial load seems to be a feasible mechanism – this may not have been the sole contributor to the failure of the bridge, as lateral spreading near the considered pile is itself under question. Moreover, as reported by Yoshida *et al.* (2007) lateral spreading started after the bridge had collapsed.

Combined Effect of Liquefaction, Axial Load and the Aftershocks at about 70 seconds

Figure 11 shows the acceleration information recorded from the basement of the Kawasgichi-Cho apartment which is about 2 km from Showa Bridge. This plot also shows the window when the Showa Bridge collapsed. It may be observed that there is slight increase in acceleration i.e. a shock wave or a jolt. It has been hypothesised, see Kudo *et al* (2000) and Yoshida *et al* (2007) that this shock wave or the jolt is from the same earthquake source and travelled the same path.

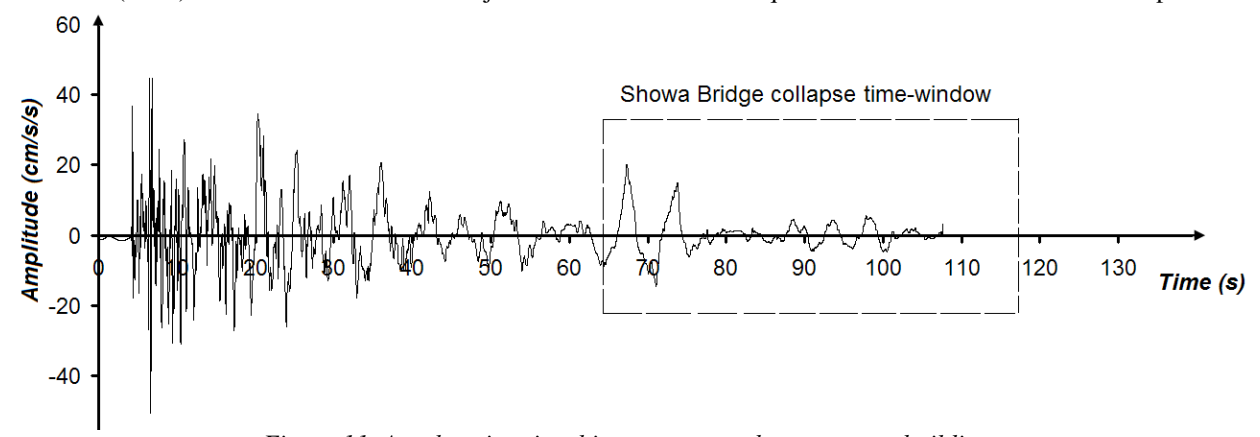


Figure 11. Acceleration time history at a nearby apartment building.

The numerical analysis carried out by Halder *et al* (2008) supports the study of Yoshida and Kudo (2000) that the liquefaction at the site occurred at about 12 seconds. After this instant, the pile can be considered to be unsupported in the liquefied zone i.e. the pile can be modelled as a long slender column. The superstructure of the Showa Bridge (i.e. the bridge decks) were composed of panels, each alternatively resting on roller and fixed supports, see Figure 12. The construction of the bridge was such that one end of the girders was locked and the other end was free to slide longitudinally off the piers except pier P6 which had both on roller supports. As discussed by Yoshida *et al* (2007), the predominant period of pier P6 would be different from the other such piers. It is reported that the seating length of the bridge pier was only 30 cm. The next section discusses two related issues:

- a) Effect of liquefaction and axial load (740 kN from the deck) on pile head displacement due to inevitable lateral perturbations.
- b) Effect of change in first natural frequency of the pile-soil-superstructure system and the aftershock at about 70 seconds



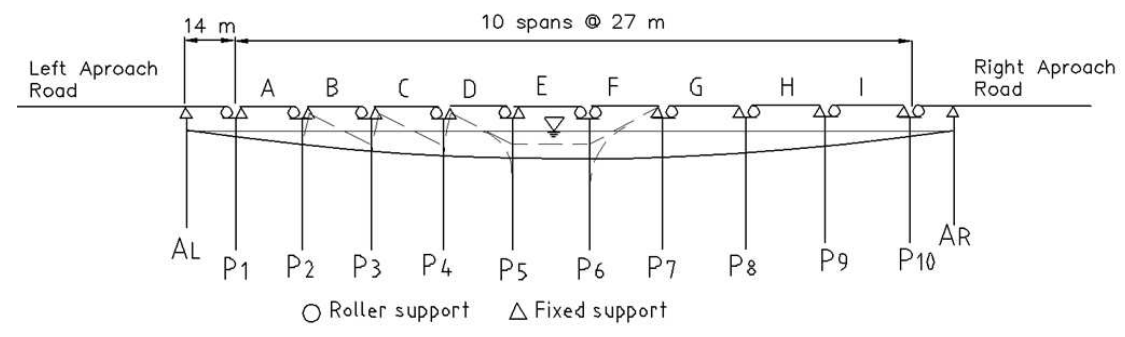


Figure 12. Support of the bridge.

Static Instability

Figure 13 shows an Euler-Bernoulli beam having a bending stiffness of EI and resting against a linear uniform elastic support of stiffness k following Bhattacharya and Adhikari (2009), Bhattacharya *et al* (2009). A constant static lateral force F is applied at the top of the beam (x=L). The well known equation of static equilibrium can be expressed as:

$$EI\frac{\partial^4 w(x)}{\partial x^4} + P\frac{\partial^2 w(x)}{\partial x^2} + kw(x) = 0$$
(3)

Where w(x) is the transverse deflection of the beam and x is the spatial coordinate along the length of the beam.

It is assumed that the mechanical properties of the beam are constant along the length. Equation (3) is a fourth-order partial differential equation and requires four boundary conditions for its solution. To comment on the pile head deflection, it is necessary to find the deflection at the top of the beam (Δ) in terms of k (soil support), P and EI.

Let Δ_0 be the deflection of the beam due to the lateral force F without the influence of the axial load and support stiffness (k). From basic mechanics,

$$\Delta_0 = \frac{FL^3}{3EI} \tag{4}$$

Figure 13. Combined pile-soil model using Euler Bernoulli beam with axial and lateral force resting against a distributed elastic support.



Equation 3 is solved for the fixed-free cantilever case and is plotted in Figure 14 in terms of non-dimensional parameters. These parameters are defined as follows:

a. Non-dimensional axial load =
$$\frac{P}{P_{cr}}$$

b. Non-dimensional support stiffness =
$$\eta = \frac{kL^4}{EI}$$

c. Buckling Amplification Factor =
$$\frac{\Delta}{\Delta_0}$$

In the above P_{cr} is the Euler Critical load for the pile given by:

$$P_{cr} = \frac{\pi^2 EI}{4I_c^2} \tag{5}$$

This value for Showa Bridge pile is computed by Bhattacharya *et al* (2005). A more general method of computing Euler buckling load for piles can be found in Bhattacharya *et al* (2004) and Bhattacharya and Madabhushi (2008).

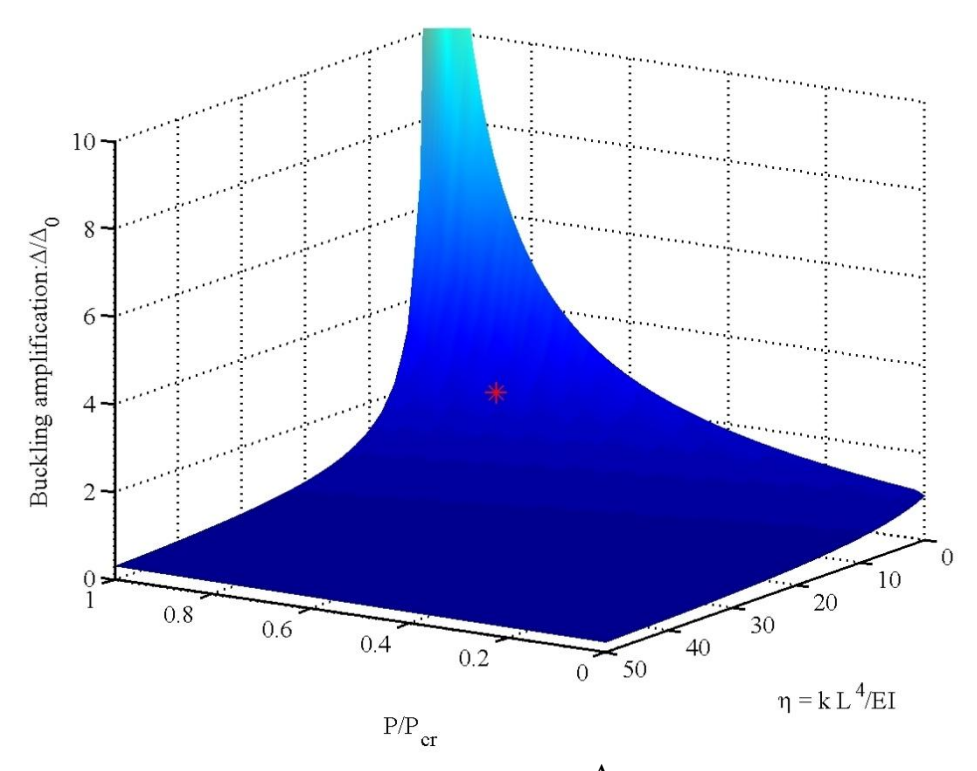


Figure 14. Variation of displacement amplification factor ($\frac{\Delta}{\Delta_0}$) due to support stiffness and axial load.

The first two parameters for the Showa Bridge case is presented in Table 2. Based on the above analysis, it can be estimated that the pile head deflection will increase by a factor of at least two times under the action of axial load. This enhanced deflection of the pile head may be adequate to dislodge the decks of the pier support. The star mark "*" in Figure 14 shows the point for Showa Bridge pile.



Table 2: Non-dimensional parameters for the Showa Bridge pile.			
Parameter	Magnitude	Remarks	
$\frac{P}{P_{cr}}$ = Non-dimensional axial load	0.82	P = 740 kN Pcr = 895 kN [Bhattacharya et al. (2005)]	
$\eta = \frac{kL^4}{EI} = \text{Non-dimensional support}$ stiffness	14000 (before earthquake) 14 (at full liquefaction)	EI = 275 MNm ² , L = 19m [k = Mean lateral pile-soil stiffness over the 10m of depth 30 MPa]. This value reduces to 0.1% at full liquefaction.	

Dynamic Instability

In addition to the above, the frequency of a bridge deck-pile-soil system will change with the liquefaction-induced stiffness degradation of the soil surrounding the pile; see for example the analytical work carried out by Adhikari and Bhattacharya (2008), Bhattacharya *et al* (2009). Usually, the time period of vibration of a pile-supported structure is estimated based on formulas which are derived from internationally calibrated data; see Chopra and Goel (2000). This time period depends on the dimension of the superstructure without any consideration to the foundation. However, during and after liquefaction, as the pile loses its lateral confinement, it becomes an integral part of the superstructure. The frequency of the structure may alter substantially and in most cases will reduce. Reduction in fundamental frequency of the structure will increase its flexibility and the structure may suffer more lateral deformation. The bending moment in the piles may increase significantly if the altered natural frequency of structure comes close to the driving frequency of the earthquake. Figure 15 shows the results of the analysis of a cantilever pile where the variation of the first natural frequency (ω_1) is plotted with respect to the normalized support stiffness (η) and the normalized axial load (P/P_{cr}), where P_{cr} is the Euler's critical buckling load.

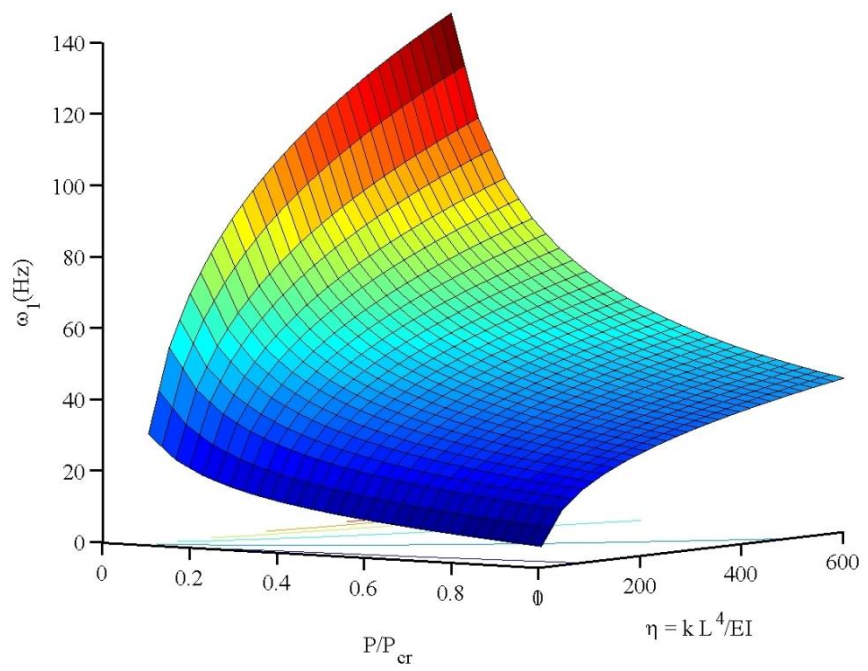


Figure 15: Variation of the first natural frequency of the cantilever pile with respect to the normalized support stiffness for different values of axial load.



Fukuoka (1966) reports the time period of the bridge is about 2 seconds. A simple estimate shows that at full liquefaction, the time period of the bridge increases by about 3 times (i.e., about 6 seconds). As the bridge failed at about 70 seconds, it is more likely that the peak in the acceleration time history possibly due to aftershock triggered an increased pile head displacement which got amplified due to the P-delta effect resulting in dislodging of the deck of pier P_6 . The other decks followed soon after.

FINAL DISCUSSION AND CONCLUDING REMARKS

The collapse of Showa Bridge during the 1964 Niigata earthquake has been, throughout the years, an iconic case study for demonstrating the devastating effects of liquefaction. Inertial forces during the initial shock (within the first 7 seconds of the earthquake) or lateral spreading of the surrounding ground (started at 83 seconds after the start of the earthquake) cannot explain the failure of Showa Bridge as the bridge failed at about 70 seconds following the main shock and before the lateral spreading of the ground started. This study showed the importance of the effects of axial load and the effect of dynamics. Quantitative analysis is carried out for the various failure mechanisms that may have contributed to the failure. This example of bridge failure can also be particularly important from the point of view of calibration of pile design methods and failure theories due to the following reasons:

- 1. This bridge collapsed just 15 days after construction, and had steel tubular piles. This ensures less uncertainty in material strength, as degradation of piles due to corrosion is not expected.
- 2. The case history is very well-documented by Takata *et al* (1965), Fukuoka (1966), Iwasaki (1984), Hamada (1992), Ishihara (1993) and Berrill and Yasuda (2002).
- 3. In addition, the role of in-depth study of case histories in earthquake geotechnical engineering cannot be underestimated.

ACKNOWLEDGMENTS

The first author would like to acknowledge the contributions of Professor Sondipon Adhikari in solving this problem.

REFERENCES

- API (2000). "Recommended Practice for planning designing and constructing Fixed Offshore Platforms." American Petroleum Institute.
- Abdoun, T. and Dobry, R. (2002). "Evaluation of pile foundation response to lateral spreading." Soil Dynamics and Earthquake Engineering, 22, 1051-1058.
- Adhikari, S. and Bhattacharya, S. (2008). "Dynamic instability of pile-supported structures in liquefiable soils during earthquakes." Shock and Vibration, IOS Press, 15(6), 665-685.
- Berrill, J. and Yasuda, S. (2002). "Liquefaction and piled foundations: Some issues." Journal of Earthquake Engineering, Vol. 6, Special Issue 1.1-41.
- Bhattacharya, S., Adhikari, S., Alexander, N.A. (2009). "A simplified method for unified buckling and free vibration analysis of pile-supported structures in seismically liquefiable soils." Soil Dynamics and Earthquake Engineering, 29, 1220-1235.
- Bhattacharya, S., Blakeborough, A., Dash, S.R. (2008). "Learning from collapse of piles in liquefiable soils." Proc., Institution of Civil Engineering, Special Issue of Civil Engineering, 161, 54-60.
- Bhattacharya, S., and Madabhushi, S.P.G. (2008). "A critical review of the methods for pile design in seismically liquefiable soils." Bulletin of Earthquake Engineering (Springer). Available online (June 2008), DOI 10.1007/s10518-008-9068-3.
- Bhattacharya, S., and Adhikari, S. (2007). "Dynamic behaviour of piled foundations in liquefiable soils during strong earthquakes." Chapter 6, "Design of foundations in seismic areas: Principles and Applications", Bhattacharya (ed), pp. 299-318, NICEE, India.
- Bhattacharya, S., Bolton, M.D., and Madabhushi, S.P.G. (2005). "A reconsideration of the safety of piled foundations in liquefied soils." Soils and Foundation, 45(4), 13-24.
- Bhattacharya, S., Madabhushi, S.P.G., and Bolton, M.D. (2004). "An alternative mechanism of pile failure in liquefiable deposits during earthquakes." Geotechnique, 54(3), 203-213.
- Bhattacharya, S. (2003). "Pile Instability during Earthquake Liquefaction." PhD thesis, University of Cambridge (U.K). September 2003.
- Bhattacharya, S & Goda, K (2013), "Probabilistic pile foundation stability analysis in liquefiable soils against buckling failure mechanism". Soil Dynamics and Earthquake Engineering, vol 45., 13-24.



The Journal's Open Access Mission is generously supported by the following Organizations:









Access the content of the ISSMGE International Journal of Geoengineering Case Histories at: https://www.geocasehistoriesjournal.org

Downloaded: Tuesday, December 02 2025, 18:11:23 UTC